

# Inflammation dynamics of atopic dermatitis: phase transition and scaling law of remission time

Yoseb Kang,<sup>1,\*</sup> Jaewoo Hwang,<sup>2,\*</sup> Yong Hyun Jang,<sup>3</sup> Ying-Cheng Lai,<sup>4,5</sup> and Younghae Do<sup>2,†</sup>

<sup>1</sup>*Department of Mathematics, Institute for Future Earth,  
Pusan National University, Busan, 46241, Republic of Korea*

<sup>2</sup>*Department of Mathematics, Nonlinear Dynamics & Mathematical Application Center,  
Kyungpook National University, Daegu, 41566, Republic of Korea*

<sup>3</sup>*Department of Dermatology, School of Medicine, Kyungpook National University, Daegu, 41944, Republic of Korea*

<sup>4</sup>*School of Electrical, Computer and Energy Engineering, Arizona State University, Tempe, 85287, USA*

<sup>5</sup>*Department of Physics, Arizona State University, Tempe, 85287, USA*

(Dated: February 24, 2025)

Atopic dermatitis (AD) is a prevalent skin disorder affecting individuals globally, with many patients experiencing a range of symptoms. While it is not life-threatening, those with milder forms of the disease often remain in a persistent disease state without full recovery. A pronounced clinical phenomenon associated with AD is the cyclic alternation of two distinct phases in time: inflammation and remission, depending on patients' immune response and skin permeability. Frequent and relatively long inflammatory times lead to symptoms that can severely deteriorate the quality of life for the patient. Through mathematical modeling, we find that patients with similar AD symptoms can be categorized into two phases depending on the skin permeability and immune response that constitute the most clinically relevant parameter plane: the inflammatory time is shorter or longer than the remission time, respectively and the transition between the two phases is of the second-order type. In the parameter plane, a critical threshold curve emerges, which separates the two phases. Computing the frequency and duration of the inflammatory response, we uncover a logarithmic scaling law governing the inflammatory and remission times and discuss its clinical implications. In particular, when the skin condition is managed such that the system is close to the phase transition point, the benefits of treatment are more pronounced. However, at this stage, the effectiveness of skincare in reducing flare-ups tends to be less noticeable, making it difficult to evaluate the success of the treatment, largely due to the nature of logarithmic decay in the remission time. Our computational study leads to insights into the mechanisms of AD that can be used to improve the diagnostic accuracy and treatment.

## I. INTRODUCTION

Utilizing the principles and methodologies of nonlinear dynamics for understanding diseases has a long history [1, 2]. The pioneering work by Glass and Mackey proposed that certain physiological disorders may be understood as dynamical diseases [3], where the diseases are viewed as the manifestation of often sudden qualitative changes in the dynamics of the underlying physiological control mechanism [4, 5]. Another extensively studied dynamical disease is epilepsy [6, 7], where the occurrence of an epileptic seizure is believed to be related to the onset of some kind of synchrony or hypersynchrony among the neurons in certain brain regions [8]. There is extensive literature on applying nonlinear dynamics to analyzing and understanding the mechanism of epilepsy, including those based on the Lyapunov exponents [9, 10], the correlation dimension [11], and phase synchronization [12].

In this paper, we apply nonlinear dynamics to a major class of human skin diseases: atopic dermatitis (AD). It is a prevalent skin condition influenced by the complex interplay among genetic, immunological, and environmental factors [13]. The disease manifests differently across various age groups, ethnicity, and genders, making it difficult to develop universally

effective methods of treatment [14–20]. Another complicating issue is the absence of reliable animal models, making it difficult for turning research findings into clinical therapeutic methods. Recently, *in-vivo*, *in-vitro*, and *in-silico* approaches have been developed for understanding the pathophysiological mechanisms underlying AD [21–26]. These methods also aim to identify key therapeutic targets and biomarkers. AD evolves continuously in time and there are different clinical stages of AD, which can thus be viewed as the result of the evolution of a nonlinear, nonautonomous dynamical system with time-varying parameters. As such, mathematical and computational models can play a role in understanding the underlying disease mechanism [24–26].

Investigating the AD progression in time is critical to understanding the underlying mechanisms of the disease and developing treatments. A key clinical manifestation of AD is inflammation, also known as the inflammatory response. It is a biological reaction of the immune system triggered by various factors such as pathogens, damaged cells, and toxic substances [20, 27, 28], which plays a crucial role in the body's immune defenses. Common symptoms of inflammation include swelling, heat, and pain. Patients with AD frequently experience recurring inflammatory responses and their daily lives consist of alternating periods of inflammatory responses and periods without such responses. The time during which an inflammatory response occurs is the inflammatory time, denoted as  $\tau_I$ , while the period without an inflammatory re-

---

\* These two authors contributed equally

† Corresponding author; [yhdo@knu.ac.kr](mailto:yhdo@knu.ac.kr)

sponse is the remission time  $\tau_R$ . From the standpoint of dynamics, the daily lives of patients with AD involve oscillations between the inflammatory and remission periods, as pictorially illustrated in Fig. 1(a). The duration and intensity of these inflammatory episodes can vary among patients with the same AD phenotype, influenced by individual factors such as the immune response levels and skin permeability [24, 25]. This raises a basic question: what roles do the inflammatory oscillation patterns play in the symptoms, phenotype, and progression of AD?

A necessary step towards addressing this question is to obtain information about the inflammatory response time. Measuring the duration of the inflammatory response in AD using the traditional *in-vivo* and *in-vitro* methods is challenging. Realistically, it is infeasible to track the inflammatory response in AD patients with various symptoms over an extended period of time. To overcome this difficulty, we shall adopt an *in-silico* approach by which the inflammatory response time is simulated using the recently developed mathematical model for AD [24–26] based on a reasonable description of the characteristics of the disease. A pioneering model was proposed based on the mechanisms underlying the pathogenesis of AD, including genetic defects in skin barrier function and immune cell activity related to barrier dysfunction [24]. In this regard, *In silico* computational experiments utilizing various nominal values corresponding to the human body functions associated with AD have provided valuable insights into the progression of the disease over time. Especially, through a dynamical analysis of AD model, four stages of AD with distinct symptoms were identified: recovery, chronic damage, mild oscillations, and severe oscillations [24–26].

Our present study focuses on the characteristics of inflammatory and remission times under different physiological/biological conditions. Two key parameters can be used to characterize these conditions: the skin permeability  $\kappa_p$  and the immune response  $\alpha_I$ . We set out to investigate how  $\tau_I$  and  $\tau_R$  vary on the parameter plane  $(\kappa_p, \alpha_I)$ , with a special eye towards the mild and severe oscillations of the AD symptoms. The main findings of this work are as follows. Patients with similar AD symptoms can be categorized into two phases in the parameter plane: the inflammatory time is shorter or longer than the remission time:  $\tau_I < \tau_R$  or  $\tau_I > \tau_R$ , respectively. A critical threshold curve arises in the parameter plane, with the behaviors  $\tau_I < \tau_R$  or  $\tau_I > \tau_R$  occurring on the two sides of the curve. As the parameters change, the system's movement across the critical curve is effectively a second-order phase transition, as both  $\tau_I$  and  $\tau_R$  vary continuously through some critical point. A pertinent issue is the frequency and duration of the inflammatory response and the impact on the “quality of life” of the patients. Our computations reveal that the values for AD onset conditions change significantly before and after the phase transition, indicating that even in patients with similar AD symptoms, different variants can occur, depending on the skin permeability and immune response. In clinical terms, a prolonged activation of a par-

ticular switch underlying AD (the R switch - to be introduced in model description below) is indicative of an extended period during which the patient experiences symptoms such as itching and scratching, leading to an unhealthy period. Understanding the duration in which the R switch remains active or inactive within a day can be useful for determining the appropriate treatment strategy. Clinically, when the skin condition is managed such that the system is close to the phase transition point, the benefits of treatment are more pronounced. A logarithmic scaling law governing the inflammatory and remission times with parameter changes has been computationally uncovered and mathematically explained. The key clinical implication of the logarithmic scaling is that it provides a significant window of opportunity for treating the disease. Overall, our computations and analysis have generated insights into the dynamical mechanisms of AD for improving the diagnosis and treatment, giving another demonstration of the power of nonlinear dynamics in probing into human diseases to garner a mechanistic understanding.

## II. NONLINEAR DYNAMICS OF ATOPIC DERMATITIS

### A. AD modeled as a nonsmooth dynamical system

We conduct an *in-silico* study on inflammation and remission times by using the recently developed mathematical model of AD [24–26]. Figure 1(a) shows the progression of AD pathogenesis [24], highlighting the dynamical interplay between skin barrier, immune regulation, and environmental stress. Under normal conditions, small amounts of pathogens that enter through compromised skin barriers are typically contained and do not pose a significant threat. However, when the amount of pathogens exceeds a certain threshold, it activates physiological mechanisms such as toll-like receptors (TLRs) and protease-activated receptor 2 (PAR2), leading to an AD flare. The immune response involves the release of antimicrobial peptides that fight against the invading pathogens and signal various immune processes that mobilize dendritic cells to the lymph nodes. If the pathogen load decreases below a deactivation threshold, these physiological mechanisms shut off, halting the flare. Conversely, if the dendritic cell count in the lymph nodes exceeds a critical threshold, it can lead to a significant and irreversible change in the immune state, which may exacerbate the skin condition considerably.

Quantitatively, the AD mechanism can be described by the following set of nonlinear differential equations [24]:

$$\begin{aligned} \frac{dP}{dt} &= \frac{P_{\text{env}}\kappa_P}{1 + \gamma_B B(t)} - \alpha_I R(t)P(t) - \delta_P P(t), \\ \frac{dB}{dt} &= \frac{\kappa_B[1 - B(t)]}{[1 + \gamma_R R(t)][1 + \gamma_G G(t)]} - \delta_B K(t)B(t), \\ \frac{dD}{dt} &= \kappa_D R(t) - \delta_D D(t), \end{aligned} \quad (1)$$

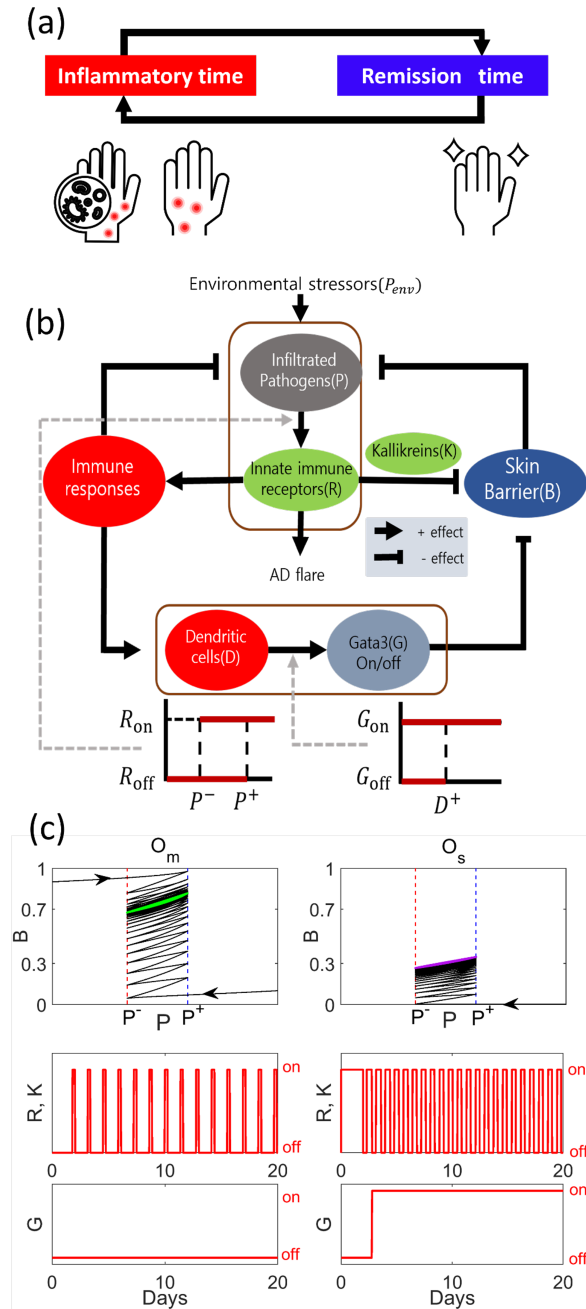


FIG. 1. AD modeled as a nonsmooth nonlinear dynamical system. (a) A cycle of processes with or without an inflammatory response. (b) A schematic representation of the processes involved in AD. (c) Oscillatory behavior of the skin barrier  $B$  over time for two *in-silico* symptoms  $O_m$  and  $O_s$ , illustrating the periods of activation (inflammatory time,  $\tau_I$ ) and inactivation (remission time,  $\tau_R$ ) of the  $R$ -switch, as well as the activation of the  $G$ -switch.

where the dynamical variables  $P(t)$ ,  $B(t)$  and  $D(t)$  represent the infiltrated pathogen load (in milligrams per milliliter), the strength of barrier integrity (relative to the maximum strength), and the concentration of dendritic cells (DCs) in the lymph node (cells per milliliter), respectively. We have

$P(t) \geq 0$ ,  $0 \leq B(t) \leq 1$  and  $D(t) \geq 0$ . The parameter values and their description are listed in Tab. II in Sec. A.

A key aspect of the AD model is the use of three switches with an on-off function to describe the inflammatory responses, which play a crucial role in the progression of AD. The three switches  $R(t)$ ,  $G(t)$  and  $K(t)$  control the levels of activated immune receptors, *Gata3* transcription (relative to the maximum transcription level), and active kallikreins, respectively, and are described as

$$R(t) = \begin{cases} R_{\text{off}}, & \text{if } P(t) < P^- \text{ or} \\ & \{P^- \leq P(t) \leq P^+, R(t^-) = R_{\text{off}}\}, \\ R_{\text{on}}, & \text{if } P(t) > P^+ \text{ or} \\ & \{P^- \leq P(t) \leq P^+, R(t^-) = R_{\text{on}}\}, \end{cases} \quad (2)$$

$$K(t) = \begin{cases} K_{\text{off}}, & \text{if } P(t) < P^- \text{ or} \\ & \{P^- \leq P(t) \leq P^+, R(t^-) = R_{\text{off}}\}, \\ m_{\text{on}}P(t) - \beta, & \text{if } P(t) > P^+ \text{ or} \\ & \{P^- \leq P(t) \leq P^+, R(t^-) = R_{\text{on}}\}, \end{cases} \quad (3)$$

$$G(t) = \begin{cases} G_{\text{off}}, & \text{if } D(t) < D^+ \text{ and } G(t^-) = G_{\text{off}}, \\ G_{\text{on}}, & \text{if } D(t) \geq D^+ \text{ or } G(t^-) = G_{\text{on}}, \end{cases} \quad (4)$$

where  $R_{\text{on}}$ ,  $R_{\text{off}}$ ,  $G_{\text{on}}$ ,  $G_{\text{off}}$  and  $K_{\text{off}}$  indicate the activating or inactivating constant-level of each switch, but only  $K_{\text{on}}$  depends on  $P(t)$ :  $K_{\text{on}} = m_{\text{on}}P(t) - \beta$ . Note that the switches  $R$  and  $K$  are hysteretic, which activate and cease AD flares. In contrast, switch  $G$  is irreversible: once activated, it remains on permanently. Because of the on-off switches, the AD model Eq. (1) constitutes a nonsmooth dynamical system with subsystems. That is, the main system can evolve into a subsystem  $S_i$  as the AD system evolves. All subsystems of the AD system Eq. (1) are described in Sec. B.

For a clinical classification of the AD phenotypes, we use the SCORAD (SCORing Atopic Dermatitis) index to evaluate the extent and severity of eczema, which is associated with cytokine levels [?]. [What is the reference here?](#) There are four classifications in SCORAD: none, mild, moderate and severe. In the *in-silico* study of AD, four attractors of AD were found [24–26]: Recovery ( $R$ ), Mild Oscillation ( $O_m$ ), Serious Oscillation ( $O_s$ ) and Chronic damage ( $C$ ).

## B. Oscillation states associated with AD

The two attractors, namely  $R$  and  $C$ , do not exhibit any oscillatory behaviors: their skin integrity correspond to  $B = 1$  (healthy skin state) and  $B = 0$  (severe damage in skin), respectively. However, the attractors  $O_m$  and  $O_s$  present oscillating behavior in skin integrity, providing insights into the dynamical evolution of AD and treatment. In particular, depending on responses of inflammation or activation of the immune receptors, either  $O_m$  or  $O_s$  can arise. Figure 2(a) shows the onset conditions [25] of  $O_m$  (red) and  $O_s$  (blue) with respect to the parameters  $\kappa_p$  and  $\alpha_I$ . In the overlapping region of two onset conditions, the outcomes can be either  $O_m$  or  $O_s$ , depending

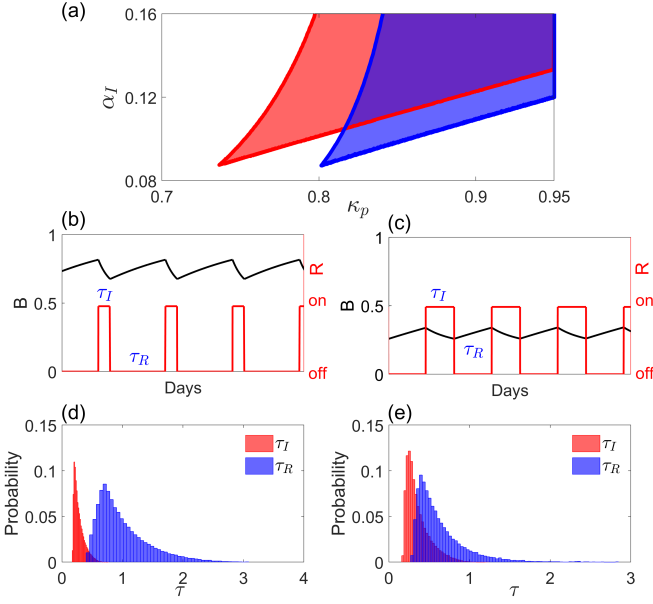


FIG. 2. Two distinct AD oscillation states. (a) Onset conditions for  $O_m$  (blue) and  $O_s$  (red) in the  $(\kappa_p, \alpha_I)$  space. (b,c) Cycles of inflammatory and remission times, along with the corresponding skin barrier  $B$  for  $O_m$  and  $O_s$ , respectively. (d,e) Distributions of inflammatory and remission times observed under the corresponding onset conditions for  $O_m$  and  $O_s$ , respectively.

on the initial condition. To study the oscillating behavior of AD in a concrete way, we focus on the parameter region highlighted by the two colors in Fig. 2(a). For a fixed parameter pair  $(\kappa_p, \alpha_I)$  in this region, the steady-state attractors  $R$  and  $C$  might also arise due to the multistability [25]. Figure 1(c) shows, for  $\kappa_p = 0.85$  and  $\alpha_I = 0.13$ , the oscillating behaviors from the attractors  $O_m$  and  $O_s$ . The corresponding switch activation is illustrated in Fig. 1(c). The skin integrity of mild oscillatory attractor  $O_m$ , shown on the left in Fig. 1(b), is close to a healthy state ( $B = 1$ ), while the attractor  $O_s$  with serious oscillations, shown on the right in Fig. 1(b), approaches chromatic damage ( $B = 0$ ). A difference between the two oscillatory attractors is activation of the  $G$  switch, as shown in Fig. 1(c), where the state of  $G$  switch of  $O_m$  ( $O_s$ ) is always off (on), respectively.

How do the oscillatory states  $O_m$  and  $O_s$  emerge? The subsystems involved in the creation of  $O_m$  are  $S_1$  and  $S_3$ . In particular, when  $S_1$  is activated, AD progresses to a healthy state. However, the  $S_3$ -subsystem leads to a progression of AD when its inflammatory response is triggered ( $R$  and  $K$  switches turned on). The oscillating behavior of  $O_m$  thus results from the repeated involvement of the subsystems:  $S_1 \rightleftharpoons S_3$ , from periodic inflammation and remission of AD. Similarly,  $O_s$  is generated by utilizing different subsystems:  $S_2 \rightleftharpoons S_4$  when the  $G$ -switch is turned on (Tab. I). That is, periodic inflammatory responses in AD, combined with an activated immune response, contribute to the emergence of  $O_s$ . As a general rule, the oscillatory behavior consists of a repetition between

Property	$O_m$	$O_s$	Time
Value of $B$	high	low	
$R, K$ -switches	off $\rightleftharpoons$ on	off $\rightleftharpoons$ on	$\tau_R \rightleftharpoons \tau_I$
$G$ -switch	off	on	
Subsystems of AD	$S_1 \rightleftharpoons S_3$	$S_2 \rightleftharpoons S_4$	

TABLE I. Properties of  $O_m$  and  $O_s$  from a dynamical point of view

a *inflammatory time*  $\tau_I$  ( $R$  and  $K$  switches-on) and a *remission time*  $\tau_R$  ( $R$  and  $K$  switches-off) of AD. Understanding these oscillatory states is crucial for more accurate prediction of the clinical outcome and for improving the quality of life in patients with AD.

### III. EMERGENCE OF PHASE TRANSITION AND SCALING LAWS GOVERNING INFLAMMATORY AND REMISSION TIMES

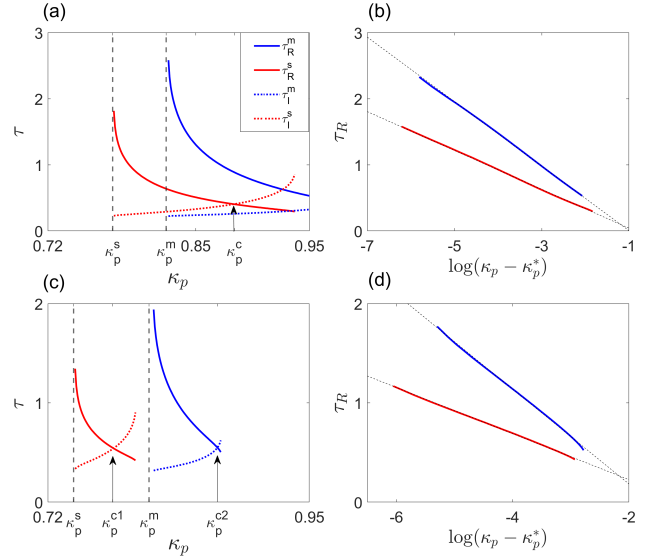


FIG. 3. Comparison of inflammatory and remission times. (a) Inflammatory and remission times  $\tau_{I,R}^{m,s}$  versus  $\kappa_p$  for  $\alpha_I = 0.13$ , where two dashed lines denote the critical onset points:  $\kappa_p^m$  and  $\kappa_p^s$ . The red and blue colors represent the inflammatory and remission times for  $O_s$  and  $O_m$ , respectively. (b) Scaling of the remission time on logarithmic and linear scales for  $\alpha_I = 0.13$ . The critical onset point  $\kappa_p^s$  corresponds to  $\kappa_p^m$  for  $O_s$  and  $\kappa_p^s$  for  $O_m$ . (c,d) Similar to (a,b), respectively, but for  $\alpha_I = 0.1$ .

#### A. Comparison of inflammatory and remission times and clinical significance

When the inflammatory response of AD as triggered by the  $R$  and  $K$ -switches is activated, commonly the patients will experience pain or discomfort due to symptoms such as itching

and scratching. During the time periods without inflammation, the skin begins to heal towards a return to the healthy state. The characteristics of the inflammatory and remission times are mainly determined by the parameters  $\kappa_p$  and  $\alpha_I$ . Understanding the relationship between two different times and their scaling behaviors is critical for both clinical assessment and therapeutic decision-making.

Based on the fact that AD patients with different nominal values ( $\kappa_p, \alpha_I$ ) can show the same symptoms, we investigate the inflammatory and remission times in terms of the onset conditions of the two oscillating states  $O_m$  and  $O_s$ , represented by the blue and red colored parameter regions in Fig. 2(a), respectively. Figures 2(b) and 2(c) present the cycles of inflammatory and remission times, along with the corresponding skin barrier  $B$  for  $O_m$  and  $O_s$ , respectively. Figure 2(d) presents the probabilistic distributions of  $\tau_I^m$  and  $\tau_R^m$  associated with the  $O_m$  symptoms. For  $\tau_I^m$ , the mean and variance are approximately 0.29 and 0.01, respectively, while those for  $\tau_R^m$  are 1.00 and 0.18. The relatively small variance of  $\tau_I^m$  suggests that AD patients exhibiting the  $O_m$  symptom tend to have a nearly consistent inflammatory response time. The remission time  $\tau_R^m$  demonstrates a broader distribution characterized by an exponential tail, indicating that AD patients with the  $O_m$  symptom generally experience a similar duration of pain before entering the recovery phase.

For  $O_s$ , we also examine the inflammatory and remission times associated with its onset condition, and their probabilistic distributions are shown in Fig. 2(e). Compared to the those for  $O_m$ , the two distributions exhibit a significant overlap. The mean and variance of  $\tau_I^s$  are approximately 0.36 and 0.02, respectively, while those for  $\tau_R^s$  are 0.64 and 0.10. Overall, the mean value of  $\tau_R^s$  is approximately twice of that of  $\tau_I^s$ . For  $O_m$ , the mean value of  $\tau_R^m$  is approximately four times larger than that of  $\tau_I^m$ . We also have that the mean value of  $\tau_I^m$  is slightly larger than that of  $\tau_I^s$ . These observations can be summarized as

$$\langle \tau_R^s \rangle \approx 1.77 \langle \tau_I^s \rangle, \quad \langle \tau_R^m \rangle \approx 3.51 \langle \tau_I^m \rangle, \quad \text{and} \quad \langle \tau_I^m \rangle \approx 1.26 \langle \tau_I^s \rangle,$$

indicating that AD patients with  $O_s$  endure a longer duration of pain compared to those with  $O_m$ .

### B. Phase transition and logarithmic scaling of inflammatory and remission times

We examine how the inflammatory time  $\tau_I$  and the remission time  $\tau_R$  depend on the skin permeability  $\kappa_p$  under the distinct onset conditions of  $O_m$  and  $O_s$ , for a fixed rate  $\alpha_I$  of pathogen eradication by innate immune responses. In this case, the critical onset points:  $\kappa_p^m$  for  $O_m$  and  $\kappa_p^s$  for  $O_s$ , are different, as exemplified in Fig. 2(a). For example, for  $\alpha_I = 0.13$ , we have  $\kappa_p^m \approx 0.82$  and  $\kappa_p^s \approx 0.77$ . Figure 3(a) illustrates  $\tau_{I,R}^m$  and  $\tau_{I,R}^s$  as a function of  $\kappa_p$  for the two states  $O_m$  and  $O_s$ , represented in blue and red, respectively. It can be seen that the remission time  $\tau_R$  for both types of oscillation decreases sharply as  $\kappa_p$  increases beyond the onset. In

contrast, the inflammatory time  $\tau_I$  increases as  $\kappa_p$  increases from the critical point, indicating that, as the skin integrity deteriorates, the patients begin to experience longer periods of inflammation and shorter periods of remission.

Under the onset condition of  $O_m$  with  $\alpha_I = 0.13$ , we observe that the remission time is consistently longer than the inflammatory time:  $\tau_I^m < \tau_R^m$ , suggesting that the patients with  $O_m$  spend the majority of their time in the remission phase, experiencing only occasional pain due to inflammatory responses. Clinically, the AD patients with the  $O_m$  symptoms spend a considerable amount of time during which their skin conditions improve. In contrast, for patients exhibiting the  $O_s$  symptoms, there exists a critical value  $\kappa_p^c$  beyond which the relationship between the remission and inflammatory times exchanges, as shown in Fig. 3(a). Specifically, for  $\kappa_p < \kappa_p^c$ , the inequality  $\tau_I^s < \tau_R^s$  holds. However, for  $\kappa_p > \kappa_p^c$ , this relationship reverses. We have

$$\begin{aligned} \tau_I^s &< \tau_R^s, \text{ if } \kappa_p < \kappa_p^c, \text{ and} \\ \tau_I^s &> \tau_R^s, \text{ if } \kappa_p > \kappa_p^c, \end{aligned} \quad (5)$$

signifying a second-order phase transition at  $\kappa_p^c$ . Clinically, when the skin permeability of the patients exhibiting the  $O_s$  symptom exceeds a critical threshold, they are likely to remain in an inflammatory state most of the time. As a result, patients may experience constant pain all times, compromising their quality of life.

To quantify the change in the remission time  $\tau_R$  after the onset of AD symptoms, we plot  $\tau_R$  on a logarithmic-linear scale:  $\tau_R^{m,s}$  versus  $\kappa_p - \kappa_p^*$ , where  $\kappa_p^*$  corresponds to  $\kappa_p^m$  for  $O_m$  or  $\kappa_p^s$  for  $O_s$ . The results are shown in Fig. 3(b), suggesting the following scaling laws:

$$\begin{aligned} \tau_R^m &\sim m_R \log(\kappa_p - \kappa_p^m) \text{ for } O_m, \text{ and} \\ \tau_R^s &\sim s_R \log(\kappa_p - \kappa_p^s) \text{ for } O_s, \end{aligned} \quad (6)$$

with the respective slopes  $m_R \approx -0.45$  and  $s_R \approx -0.1$ . As  $\kappa_p$  approaches the critical value  $\kappa_p^*$ , the remission time exhibits a logarithmic decay law.

What are the clinical implications of the logarithmic scaling law? To address this question, we note that the variation of the remission time for the AD patient depends on the specific AD symptoms and decrease as  $\kappa_p$  undergoes a slight change from the onset point  $\kappa_p^*$ . Because of the constraint  $m_R < s_R$ , the remission time for  $O_s$  decreases more quickly than that for  $O_m$ . For  $\kappa_p$  is far above  $\kappa_p^*$ , a reduction in the remission time occurs at a much slower rate due to the nature of the logarithmic decay, suggesting that taking care of the skin immediately after the onset of AD can significantly prolong the remission period. In contrast, when AD progresses to a stage where  $\kappa_p$  is greater than  $\kappa_p^*$ , the impact on the remission time becomes minimal. Specifically, when the skin condition is managed so that  $\kappa_p$  is close to  $\kappa_p^*$  ( $\kappa_p^* \lesssim \kappa_p$ ), the benefits of treatment are more pronounced. However, at this stage, the effectiveness of skincare in reducing flare-ups tends to be less noticeable, making it difficult to evaluate the success of the treatment, largely due to the nature of logarithmic decay in the remission time.

We now investigate the dependence of the inflammatory and remission times on  $\kappa_p$  as the immune response is reduced. For this purpose, we set  $\alpha_I = 0.1$ . The results are shown in Fig. 3(c), where there is a phase transition for both the  $O_m$  and  $O_s$  states:

$$\begin{aligned} \tau_I^m &< \tau_R^m, & \text{if } \kappa_p < \kappa_p^{c1}, & \quad \tau_I^s < \tau_R^s, & \text{if } \kappa_p < \kappa_p^{c2}, \\ \tau_I^m &> \tau_R^m, & \text{if } \kappa_p > \kappa_p^{c1}, & \quad \tau_I^s > \tau_R^s, & \text{if } \kappa_p > \kappa_p^{c2}. \end{aligned} \quad (8)$$

The scaling of the remission time remains to be logarithmic [(6)], as shown in Fig. 3(d). Considering that, at a higher level of immune response ( $\alpha_I = 0.13$ ), only the  $O_s$  state exhibits a phase transition, as shown in Fig. 3(a), we see that a reduced level of immune response can lead to a phase transition in both the  $O_m$  and  $O_s$  states.

To further explore the phase transition phenomenon between  $\tau_R$  and  $\tau_I$ , we examine these times under the onset conditions of the two oscillating states. Figures 4(a) and 4(b) illustrate the critical points of the phase transition for  $O_m$  and  $O_s$  (marked in black). Remarkably, the numerically determined critical points form a straight line, as shown by the black lines in Figs. 4(a) and 4(b):

$$\alpha_I \approx 0.253\kappa_p - 0.119, \quad \text{for } O_m, \quad \text{and} \quad (9)$$

$$\alpha_I \approx 0.283\kappa_p - 0.121 \quad \text{for } O_s. \quad (10)$$

These are the critical phase-transition line, denoted as  $P_{line}$ . For the onset condition of  $O_m$ , the critical line  $P_{line}$  is positioned close to the boundary of this condition. The proximity indicates a relatively small area below the line  $P_{line}$  in the onset condition of  $O_m$ . As a result, the AD patients with  $O_m$  are less likely to experience the phase transition. In contrast, for the onset condition of  $O_s$ , the area below the line  $P_{line}$  is significantly larger, indicating that the AD patients with  $O_s$  are more likely to experience the phase transition, which could complicate the progression of the AD symptoms. Overall, for both  $O_m$  and  $O_s$ , the inequality  $\tau_I^m < \tau_R^m$  holds in the area above the straight line, while opposite holds below the line. Consequently, depending on the immune responses  $\alpha_I$  and skin permeability  $\kappa_p$ , the order in the length of the inflammatory and remission time can be changed:

$$\tau_I^m < \tau_R^m \rightarrow \tau_R^m < \tau_I^m \quad \text{and} \quad \tau_I^s < \tau_R^s \rightarrow \tau_R^s < \tau_I^s, \quad (11)$$

implying a significant disparity in the quality of life for patients with AD, even when they exhibit similar symptoms, as characterized by the scaling relation (9).

### C. Behaviors of inflammatory response

Associated with the inflammatory response, the key dynamical variable underlying the AD, namely the strength of barrier integrity  $B(t)$ , exhibits periodic oscillations, as exemplified in Figs. 2(a) and 2(b). Each period contains a cycle of inflammation and remission. As stronger inflammatory responses

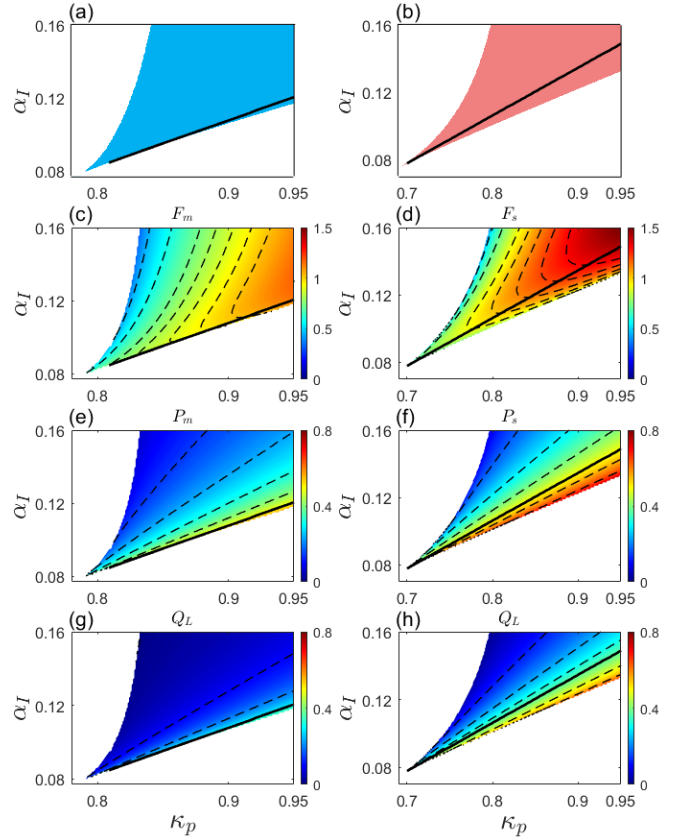


FIG. 4. Phase transition associated with the  $O_m$  and  $O_s$  states. (a,b) Critical phase-transition line  $P_{line}$  marked by black line with respect to the onset conditions of  $O_m$  and  $O_s$ , respectively. In the  $(\kappa_p, \alpha_I)$  plane, the critical points of phase transitions are indicated by the black lines on the onset conditions of  $O_m$  and  $O_s$ , corresponding to the blue and red regions, respectively.

lead to more severe AD symptoms, a question is how frequent these cycles are. To address this question, we define the frequencies of the inflammatory response for the  $O_m$  and  $O_s$  states as

$$F_m = \frac{1}{\tau_I^m + \tau_R^m} \quad \text{and} \quad F_s = \frac{1}{\tau_I^s + \tau_R^s}. \quad (12)$$

Figures 4(c) and 4(d) show the values of  $F_m$  and  $F_s$  under their respective onset conditions in the parameter plane  $(\kappa_p, \alpha_I)$ . As  $\kappa_p$  increases, the maximum frequencies occur just above the critical line  $P_{line}$ , indicating a correlation between the frequency and phase transition. Especially, when the immune response and skin permeability are near the critical line, the frequency of the inflammatory response is significantly elevated. Within each oscillatory state, the frequency distribution is wide: the ranges of  $F_m$  and  $F_s$  are (0.3, 1.2) and (0.4, 1.5), respectively.

Within a cycle, the fraction of the inflammatory time can also vary widely, depending on the parameter values. The

fractions associated with the  $O_m$  and  $O_s$  states are given by

$$P_m = \frac{\tau_I^m}{\tau_I^m + \tau_R^m} \quad \text{and} \quad P_s = \frac{\tau_I^s}{\tau_I^s + \tau_R^s}. \quad (13)$$

As  $P_{m,s}$  approaches the value 1, patients will incur persistent inflammation most of the time. Figures 4(e) and 4(f) illustrate the values of  $P_m$  and  $P_s$ , respectively, in the parameter plane  $(\kappa_p, \alpha_I)$ . Below the critical line  $P_{line}$ , the fraction of time that the system is in an inflammatory state is large, due to the occurrence of a phase transition. In general, the fractions can vary significantly, depending on the severity of the AD symptoms: the ranges of  $P_m$  and  $P_s$  are  $(0.04, 0.6)$  and  $(0.04, 0.8)$ , respectively.

Clinically, maintaining a healthy quality of life is an important goal for any AD patient, as prolonged flare-ups will significantly impact both the physical and emotional well-being. These symptomatic periods disrupt daily activities and sleep, further compounding the effects on the patient's Quality of Life (QoL). Conversely, inactivation of the R-switch represents periods of remission or reduced disease activity, during which the patients experience relief from symptoms. In general, when the condition of the skin worsens, patients experience symptoms such as itching, swelling, heat, and pain due to inflammation [28–30]. The health-related QoL for AD patients is determined by the dynamical behaviors of the oscillatory states  $O_m$  and  $O_s$ . Quantitatively, the QoL can be assessed by examining how the degree of inflammatory response varies with the skin integrity. To this end, we define a measure reflecting the QoL:

$$Q_L = (1 - \langle B \rangle) P_{m,s}, \quad (14)$$

Where  $\langle B \rangle$  is the average skin integrity throughout a cycle that includes both inflammatory and remission periods. A near zero value of  $Q_L$  indicates that the skin condition of the patients is good or that the inflammation levels are low. In contrast, as  $Q_L$  approaches one, a high level of inflammatory response can be expected, signifying poor skin conditions.

Figures 4(g) and 4(h) show the variations of  $Q_L$  in the parameter plane  $(\kappa_p, \alpha_I)$  the  $O_m$  and  $O_s$  states, respectively. While the AD symptoms may vary, a AD patient's quality of life can diminish when their skin condition falls below a critical threshold of phase transition. When the oscillations are mild ( $O_m$ ), the values of  $Q_L$  range from 0.01 to 0.4. In contrast, for the severe oscillation state  $O_s$ ,  $Q_L$  ranges from 0.01 to 0.7, indicating a more significant decline of the quality of life as compared with the case of mild oscillations.

For a fixed value of  $\kappa_p = 0.85$ , we examine how changes in the immune response parameter  $\alpha_I$  affect the inflammatory and remission times, the frequency of the inflammatory response, the fraction of time spent in inflammation, and the overall quality of life, as shown in Fig. 5. In Fig. 5, each column corresponds to one type of symptom and the dashed lines indicate the values of  $\alpha_I$  corresponding to the critical values  $\kappa_p^*$  in Fig. 4. As  $\alpha_I$  increases beyond the dashed critical line, the inflammatory time  $\tau_I$ , the fraction of time  $P_{m,s}$

spent in inflammation, and the measure  $Q_L$  of the quality of life all decrease, while the remission time  $\tau_R$  increases. This suggests that a stronger immune response is associated with better health outcomes. Notably, the local maximum of the inflammatory response frequency  $F_{m,s}$  occurs right after the critical dashed line and subsequently begins to decrease. As a result, after the phase transition, a delay arises before the frequency of the inflammatory response begins to change.

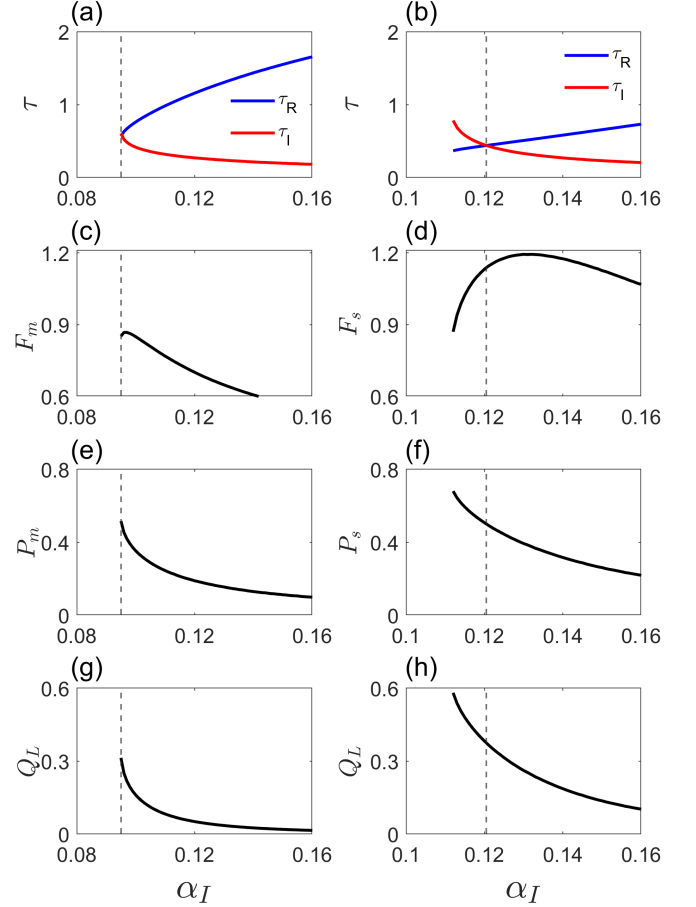


FIG. 5. Effect of varying the immune response parameter  $\alpha_I$  on the dynamics of AD. For a fixed  $\kappa_p = 0.85$ , the effects of varying  $\alpha_I$  on inflammatory and remission times (a,b), the frequency of the inflammatory response (c,d) the fraction of inflammatory time (e,f), and quality of life (g,h). The left and right columns correspond to mild and severe oscillations, respectively.

#### IV. DISCUSSION

A unique feature common to the AD disease is the emergence of oscillations. For example, as the skin conditions deteriorate, before severe damage occurs, the symptoms as determined by the strength of barrier integrity can undergo periodic cycles, with each cycle consisting of two characteristically distinct types of behaviors: inflammation and remission. During the inflammatory time, severe discomfort can

arise, making low the quality of life for the patients, whereas not much discomfort occurs during the remission time. Qualitatively, two distinct types of oscillations in the skin integrity exist among the AD patients: depending on the inflammatory and immune responses of the patient, the oscillations can be mild or severe. Regardless of the type of oscillations, to effectively reduce the inflammatory time or, equivalently, to prolong the remission time in a cycle of oscillation is a goal for treatment strategies. To achieve this goal, it is necessary to uncover the quantitative dependence of the inflammatory and remission times on the skin condition. Due to the long time span of the AD, clinical tests to determine this dependence are infeasible, and mathematical modeling provides a viable approach to gaining insights into how the inflammatory and remission times change as some parameter characterizing the skin condition changes.

The two findings of our work are: (1) the emergence of a phase transition in the inflammatory and remission times and (2) a logarithmic scaling law governing the remission time. In particular, as a key bifurcation parameter, the skin permeability, continuously increases from a small, healthy value so that the skin's barrier becomes less and less effective to protect the body from harmful substances, either mild or severe oscillations in the strength of the barrier integrity can arise, depending on the skin conditions of the individuals. At the onset of the oscillations, the remission time is much larger than the inflammatory time. As the skin permeability increases further, the remission time decreases, accompanied by a corresponding increase in the inflammatory time. At the critical value of the skin permeability, the two types are equal, after which the inflammatory time surpasses the remission time, signifying a phase transition. Since both times change continuously through the critical point, the phase transition is of the second-order type. Prior to the critical point, the discomfort is less serious. A balance between comfort and discomfort is reached at the critical point, after which the time period of discomfort exceeds that of comfort, leading to a decrease in patient's quality of life. Measuring the skin permeability parameter from the onset of the oscillations, the remission time decreases logarithmically with the parameter increment from the onset. From a clinical point of view, the logarithmic dependence is beneficial as it provides a time window for treatment or intervention.

It is worth stressing that, while the findings in this work are from mathematical modeling and a dynamical analysis of the AD, to verify the findings clinically is infeasible at the present time. For understanding the AD, mathematical model will continue to be effective to provide insights into the underpinnings of the skin disease for better treatment strategies.

#### ACKNOWLEDGMENTS

This work was supported by the National Research Foundation of Korea (NRF) grant funded by the Ko-

Parameter	Description	Value
$P_{env}$	Environmental stress load	95 (mg/mL)
$\gamma_B$	Barrier-mediated inhibition of pathogen infiltration	1
$\kappa_p$	Nominal skin permeability	(1/day)
$\alpha_I$	Rate of pathogen eradication by innate immune responses	(1/day)
$\delta_P$	Basal pathogen death rate	1 (1/day)
$\kappa_B$	Barrier production rate	0.5 (1/day)
$\gamma_R$	Innate immunity-mediated inhibition of barrier production	10
$\delta_B$	Rate of kallikrein-dependent barrier degradation	0.1
$\gamma_G$	Adaptive immunity-mediated inhibition of barrier production	1
$\kappa_D$	Rate of DC activation by receptors	4 cells/(mL 3 day)
$\delta_D$	Rate of DC degradation	0.5 (1/day)
$P^-$	Receptor inactivation threshold	26.6 (mg/mL)
$P^+$	Receptor activation threshold	40 (mg/mL)
$D^+$	<i>Gata3</i> activation threshold	85 (cells/mL)
$R_{off}$	Receptor off level	0
$R_{on}$	Receptor on level	16.7
$G_{off}$	<i>Gata3</i> off level	0
$G_{on}$	<i>Gata3</i> on level	1
$K_{off}$	Kallikrein off level	0
$m_{on}$	Slope of the linear relation between $P(t)$ and $K_{on}$	0.45
$\beta_{on}$	Y-intercept of the linear relation between $P(t)$ and $K_{on}$	6.71

TABLE II. Description and values of the parameters of the AD system Eq (1)

rean government (MSIT) (Nos. NRF-2022R1A5A1033624 & 2022R1A2C3011711). The work at Arizona State University was supported by the Air Force Office of Scientific Research through Grant No. FA9550-21-1-0438.

#### Appendix A: Parameters of AD model

Parameters of the AD system Eq. (1) and their description are listed in Tab. II.

#### Appendix B: Subsystem of AD model

Depending on status of three switches or inflammation responses, the AD model Eq. (1) can have a different form or representation, leading to the following subsystems.

$S_1$ -*subsystem*. All switches in the AD system Eq. (1) are off:  $(R, K, G) = (R_{off}, K_{off}, G_{off}) = (0, 0, 0)$ , leading to

$$\begin{aligned} \frac{dP}{dt} &= \frac{P_{env} \cdot \kappa_p}{1 + \gamma_B B(t)} - \delta_P P(t), \\ \frac{dB}{dt} &= \kappa_B [1 - B(t)], \\ \frac{dD}{dt} &= -\delta_D D(t), \end{aligned} \quad (B1)$$

*S<sub>2</sub>-subsystem.* Only the  $G$  switch is on, indicating a deficiency in the immune response:  $(R, K, G) = (R_{\text{off}}, K_{\text{off}}, G_{\text{on}} = 1)$ . The system becomes

$$\begin{aligned} \frac{dP}{dt} &= \frac{P_{\text{env}} \cdot \kappa_P}{1 + \gamma_B B(t)} - \delta_P P(t), \\ \frac{dB}{dt} &= \frac{\kappa_B [1 - B(t)]}{[1 + \gamma_G]}, \\ \frac{dD}{dt} &= -\delta_D D(t), \end{aligned} \quad (\text{B2})$$

*S<sub>3</sub>-subsystem.* Only the  $R$  and  $K$  switches are on:  $(R, K, G) = (R_{\text{on}}, K_{\text{on}}, G_{\text{off}} = 0)$ . In this case, the environment is such that a critical level of the infiltrated pathogen load is exceeded. The system becomes

$$\begin{aligned} \frac{dP}{dt} &= \frac{P_{\text{env}} \cdot \kappa_P}{1 + \gamma_B B(t)} - \alpha_I R_{\text{on}} P(t) - \delta_P P(t), \\ \frac{dB}{dt} &= \frac{\kappa_B [1 - B(t)]}{[1 + \gamma_R R_{\text{on}}]} - \delta_B K(t) B(t), \\ \frac{dD}{dt} &= \kappa_D R_{\text{on}} - \delta_D D(t), \end{aligned} \quad (\text{B3})$$

*S<sub>4</sub>-subsystem.* All switches in the AD system are on,  $(R, K, G) = (R_{\text{on}}, K_{\text{on}}, G_{\text{on}})$ , signifying the situation where the AD immune response is deficient and the environmental infiltrated pathogen load exceeds a critical level. The system equations are

$$\begin{aligned} \frac{dP}{dt} &= \frac{P_{\text{env}} \cdot \kappa_P}{1 + \gamma_B B(t)} - \alpha_I R_{\text{on}} P(t) - \delta_P P(t), \\ \frac{dB}{dt} &= \frac{\kappa_B [1 - B(t)]}{[1 + \gamma_R R_{\text{on}}][1 + \gamma_G G_{\text{on}}]} - \delta_B K(t) B(t), \\ \frac{dD}{dt} &= \kappa_D R_{\text{on}} - \delta_D D(t), \end{aligned} \quad (\text{B4})$$

### Appendix C: Logarithmic scaling governing the remission time

When the  $R$  and  $K$  switches are turned off, the remission time  $\tau_R$  represents the travel time from the point  $(P^-, B_1)$  to  $(P^+, B_2)$ , as illustrated in Fig. 6(a). Therefore, we can determine the remission time from the  $S_1$ -system, Eq. (B1), by satisfying the following conditions:

$$\begin{aligned} P(0) &= P^-, B(0) = B_1 \quad \text{at } t = 0, \\ P(\tau_R) &= P^+, B(\tau_R) = B_2 \quad \text{at } t = \tau_R. \end{aligned}$$

From Eq. (B1), we can easily find  $B(t)$ :

$$B(t) = 1 + (B_1 - 1)e^{-\kappa_B t}. \quad (\text{C1})$$

By substituting this into the equation for  $P$ , we get

$$\frac{dP}{dt} = \frac{P_{\text{env}} \cdot \kappa_P}{1 + \gamma_B [1 + (B_0 - 1)e^{-\kappa_B t}]} - \delta_P P(t). \quad (\text{C2})$$

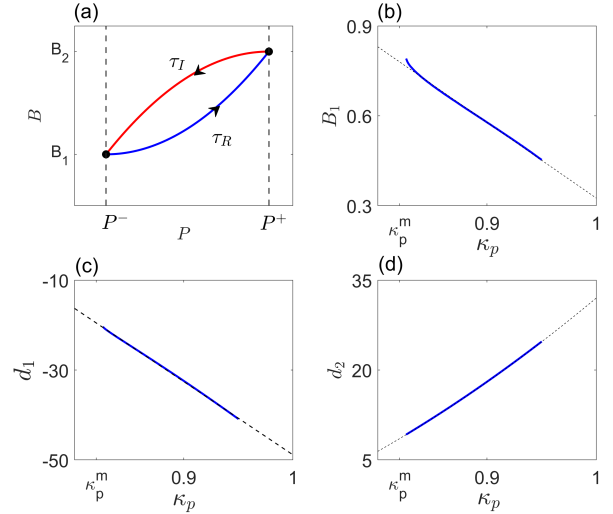


FIG. 6. (a) Illustration of oscillation between two points  $(P^-, B_1)$  and  $(P^+, B_2)$ , for the remission and inflammatory times. For the fixed value of  $\alpha_I = 0.13$ , (b-d) display the numerically calculated coefficients  $B_1$ ,  $d_1$ , and  $d_2$  associated with  $\kappa_p$ . Each dashed line (or curve) in (b-d) represents the fitted regression results.

Using the parameter values provided in Tab. II, i.e.,  $\delta_P = 1$ ,  $\gamma_B = 1$  and  $\kappa_B = 0.5$ , and then multiplying both sides by  $e^t$ , we obtain

$$\frac{d}{dt}(e^t P(t)) = e^t P'(t) + e^t P(t) = \frac{e^t}{c_1 + c_2 e^{-t/2}}, \quad (\text{C3})$$

where  $c_1 = \frac{2}{P_{\text{env}} \kappa_P}$  and  $c_2 = \frac{(B_0 - 1)}{P_{\text{env}} \kappa_P}$ . Thus, we get

$$P(t) = e^{-t} \left( \int \frac{e^x}{c_1 + c_2 e^{-x/2}} dx \right) \equiv e^{-t} I(t). \quad (\text{C4})$$

Let  $u(t) = c_1 e^{t/2} + c_2$ , then  $I(t)$  can be calculated by the following way:

$$\begin{aligned} I(t) &= \int \frac{e^x}{c_1 + c_2 e^{-x/2}} dx = \int \frac{e^{3x/2}}{c_1 e^{x/2} + c_2} dx \\ &= \int \left( \frac{u - c_2}{c_1} \right)^3 \frac{1}{u} \frac{2}{c_1} \frac{c_1}{u - c_2} du \\ &= \frac{2}{c_1^3} \left( (c_1 e^{t/2} + c_2)^2 / 2 - 2c_2(c_1 e^{t/2} + c_2) \right. \\ &\quad \left. + c_2^2 \log |c_1 e^{t/2} + c_2| \right) + C, \end{aligned}$$

where  $C$  is a constant of integration. Using the initial condition  $P(0) = P^-$ , we can determine the constant,  $C$ :

$$C = P^- - \frac{2}{c_1^3} \left\{ \frac{(c_1 + c_2)^2}{2} - 2c_2(c_1 + c_2) + c_2^2 \log |c_1 + c_2| \right\}.$$

Therefore, we finally obtain  $P(t)$  as the following form from Eq. (C4):

$$P(t) = e^{-t}I(t) = d_1e^{-t} + d_2e^{-t/2} + d_3, \quad (\text{C5})$$

where

$$d_1 = \frac{2}{c_1^3} \left\{ -\frac{3c_2^2}{2} + \frac{c_1^3}{2}C + c_2^2 \log(c_1e^{t/2} + c_2) \right\}, \quad (\text{C6})$$

$$d_2 = -\frac{2c_2}{c_1^2} = \frac{1}{2}(1 - B_1)P_{env}\kappa_p, \quad (\text{C7})$$

$$d_3 = \frac{1}{c_1} = \frac{P_{env}\kappa_p}{2}. \quad (\text{C8})$$

Since the remission time  $\tau_R$  is a solution that satisfies  $P(\tau_R) = P^+$ , we need to solve the following algebraic equation:

$$P^+ = d_1T^2 + d_2T + d_3, \quad (\text{C9})$$

where  $T = e^{-t/2}$ . Equation (C9) is implicit because the coefficient  $d_1$  depends on the variable  $t$  and  $B_1$  is determined by its relationship with  $\kappa_p$ . making it infeasible to obtain an analytic solution. We thus resort to numerically solving the coefficients  $B_1$ ,  $d_1$ , and  $d_2$  using the data  $\tau_R$  in Fig. 3 with the fixed  $\alpha_I = 0.13$ . The results are illustrated in Figs. 6(b-d). In particular, Figs. 6(c) and 6(d) demonstrate that  $d_1$  has a linear relationship with  $\kappa_p$  and  $d_2$  exhibits a quadratic relationship,

with the correlation coefficients of  $R^2 = 0.9998$  and  $R^2 = 1$ , respectively. These relations enable us to express the coefficients in the following forms:

$$d_1 = m_1\kappa_p + n_1, \quad (\text{C10})$$

$$d_2 = m_2\kappa_p^2 + n_2\kappa_p,$$

where  $m_1 \approx -163.1$ ,  $m_2 \approx 120$ ,  $n_1 \approx 114.2$  and  $n_2 \approx -87.97$ . For different values of  $\alpha_I$ , we have verified that the coefficients  $d_1$  and  $d_2$  retain the same form as in Eq. (C10).

Solving Eq. (C9) for  $T$ , we obtain:

$$T = \frac{-d_2 + \sqrt{d_2^2 - 4d_1d_3}}{2d_1}, \quad (\text{C11})$$

where  $d_4 = d_3 - P^+$  and can be expressed as  $m_4\kappa_p + n_4$ . Since the numerator of  $T$  is a quadratic function of  $\kappa_p$  and the denominator is a linear function, the dependence of  $T$  on  $\kappa_p$  is linear:

$$T \sim a\kappa_p - b, \quad (\text{C12})$$

where  $a$  and  $b$  are constants. Since  $T = e^{-\tau_R/2}$ , we obtain the logarithmic scaling law between  $\tau_R$  and  $\kappa_p$ :

$$\tau_R \sim -2\log(\kappa_p - c), \quad (\text{C13})$$

where  $c$  is a constant.

- 
- [1] L. Glass and M. C. Mackey, *From Clocks to Chaos: The Rhythms of Life* (Princeton University Press, Princeton, NJ, 1988).
- [2] D. Kaplan and L. Glass, *Understanding Nonlinear Dynamics* (Springer-Verlag, Berlin, 1995).
- [3] J. Belair, L. Glass, U. an der Heiden, and J. Milton, Dynamical disease: Identification, temporal aspects and treatment strategies for human illness, *Chaos* **5**, 1 (1975).
- [4] M. C. Mackey and L. Glass, Oscillation and chaos in physiological control systems, *Science* **197**, 287 (1977).
- [5] L. Glass and M. C. Mackey, Pathological conditions resulting from instabilities in physiological control systems, *Ann. NY Acad. Sci.* **316**, 214 (1979).
- [6] J. Milton and P. Jung, *Epilepsy as a Dynamic Disease* (Springer, New York, 2003).
- [7] I. Osorio, M. G. Frei, D. Sornette, J. Milton, and Y.-C. Lai, Epileptic seizures: Quakes of the brain?, *Phys. Rev. E* **82**, 021919 (2010).
- [8] E. R. Kandel, J. D. Koester, S. H. Mack, and S. A. Siegelbaum, *Principles of Neural Science*, sixth ed. (McGraw Hill, New York, 2021).
- [9] Y.-C. Lai, M. A. F. Harrison, M. G. Frei, and I. Osorio, Inability of lyapunov exponents to predict epileptic seizures, *Phys. Rev. Lett.* **91**, 068102 (2003).
- [10] Y.-C. Lai, M. A. F. Harrison, M. G. Frei, and I. Osorio, Controlled test for predictive power of lyapunov exponents: their inability to predict epileptic seizures, *Chaos* **14**, 630 (2004).
- [11] M. A. F. Harrison, I. Osorio, M. G. Frei, S. Asuri, and Y.-C. Lai, Correlation dimension and integral do not predict epileptic seizures, *Chaos* **15**, 033106 (2005).
- [12] Y.-C. Lai, M. G. Frei, I. Osorio, and L. Huang, Characterization of synchrony with applications to epileptic brain signals, *Phys. Rev. Lett.* **98**, 108102 (2007).
- [13] D. Y. Leung, Atopic dermatitis: new insights and opportunities for therapeutic intervention, *J. Allergy Clin. Immunol.* **105**, 860 (2000).
- [14] K. Abuabara, D. J. Margolis, and S. M. Langan, The long-term course of atopic dermatitis, *Dermatol. Clin.* **35**, 291 (2017).
- [15] L. Paternoster, O. E. Savenije, J. Heron, D. M. Evans, J. M. Vonk, B. Brunekreef, A. H. Wijga, A. J. Henderson, G. H. Koppelman, and S. J. Brown, Identification of atopic dermatitis subgroups in children from 2 longitudinal birth cohorts, *J. Allergy Clin. Immunol.* **141**, 964 (2018).
- [16] S. Illi, E. von Mutius, S. Lau, R. Nickel, C. Grüber, B. Niggemann, U. Wahn, and M. A. S. G. et al., The natural course of atopic dermatitis from birth to age 7 years and the association with asthma, *J. Allergy Clin. Immunol.* **113**, 925 (2004).
- [17] D. Garmhausen, T. Hagemann, T. Bieber, I. Dimitriou, R. Fimmers, T. Diepgen, and N. Novak, Characterization of different courses of atopic dermatitis in adolescent and adult patients, *Allergy* **68**, 498 (2013).
- [18] C. Roduit, R. Frei, M. Depner, A. M. Karvonen, H. Renz,

- C. Braun-Fahrländer, E. Schmausser-Hechfellner, J. Pekkanen, J. Riedler, and J. e. a. Dalphin, Phenotypes of atopic dermatitis depending on the timing of onset and progression in childhood, *JAMA Pedia*. **171**, 655 (2017).
- [19] Y. J. Kim, S. J. Yun, J.-B. Lee, S. J. Kim, Y. H. Won, and S.-C. Lee, Four years prospective study of natural history of atopic dermatitis aged 7–8 years at an individual level: a community-based survey by dermatologists' skin examination in childhood, *Ann. Dermatol.* **28**, 684 (2016).
- [20] E. Vakirlis, E. Lazaridou, T. Tzellos, S. Gerou, D. Chatzidimitriou, and D. Ioannides, Investigation of cytokine levels and their association with scorad index in adults with acute atopic dermatitis, *Journal of the European Academy of Dermatology and Venereology* **25**, 409 (2011).
- [21] R. J. Tanaka and M. Ono, Skin disease modeling from a mathematical perspective, *J. Investi. Dermatol.* **133**, 1472 (2013).
- [22] D. Bending and M. Ono, Interplay between the skin barrier and immune cells in patients with atopic dermatitis unraveled by means of mathematical modeling, *J. Allergy Clin. Immunol.* **139**, 1790 (2017).
- [23] K. Eyerich, S. J. Brown, B. E. P. White, R. J. Tanaka, R. Bissonette, S. Dhar, T. Bieber, D. J. Hijnen, E. Guttman-Yassky, and A. e. a. Irvine, Human and computational models of atopic dermatitis: A review and perspectives by an expert panel of the International Eczema Council, *J. Allergy Clin. Immunol.* **143**, 36 (2019).
- [24] E. Domínguez-Hüttinger, P. Christodoulides, K. Miyauchi, A. D. Irvine, M. Okada-Hatakeyama, M. Kubo, and R. J. Tanaka, Mathematical modeling of atopic dermatitis reveals "double-switch" mechanisms underlying 4 common disease phenotypes, *J. Allergy Clin. Immunol.* **139**, 1861 (2017).
- [25] Y. Kang, E. H. Lee, S. Kim, Y. H. Jang, and Y. Do, Complexity and multistability of a nonsmooth atopic dermatitis system, *Chaos Soli. Frac.* **153**, 111575 (2021).
- [26] Y. Kang, J. Hwang, Y.-C. Lai, H. Choi, and Y. Do, A nonlinear transient-dynamics approach to atopic dermatitis: Role of spontaneous remission, *Chaos Soli. Frac.* **179**, 114464 (2024).
- [27] E. Guttman-Yassky, J. G. Krueger, and M. G. Lebwohl, Systemic immune mechanisms in atopic dermatitis and psoriasis with implications for treatment, *Exp. Dermatol.* **27**, 409 (2018).
- [28] M. Furue and T. Kadono, "inflammatory skin march" in atopic dermatitis and psoriasis, *Inflamm. Res.* **66**, 833 (2017).
- [29] M. Furue and T. Kadono, New therapies for controlling atopic itch, *J. Dermatol.* **42**, 847 (2015).
- [30] J. G. Holm, T. Agner, M.-L. Clausen, and S. F. Thomsen, Quality of life and disease severity in patients with atopic dermatitis, *J. Euro. Acad. Dermatol. Venereol.* **30**, 1760 (2016).